



Analytical results for a minimalist thermal diodeLucianno Defaveri ¹ and Celia Anteneodo ^{1,2}¹*Department of Physics, PUC-Rio, Rio de Janeiro, 22453-900 RJ, Brazil*²*Institute of Science and Technology for Complex Systems, Rio de Janeiro, Brazil*

(Received 4 May 2021; accepted 15 June 2021; published 6 July 2021)

We consider a system consisting of two interacting classical particles, each one subject to an on-site potential and to a Langevin thermal bath. We analytically calculate the heat current that can be established through the system when the bath temperatures are different, for weak nonlinear forces. We explore the conditions under which the diode effect emerges when inverting the temperature difference. Despite the simplicity of this two-particle diode, an intricate dependence on the system parameters is put in evidence. Moreover, behaviors reported for long chains of particles can be extracted, for instance, the dependence of the flux with the interfacial stiffness and type of forces present, as well as the dependencies on the temperature required for rectification. These analytical results can be a tool to foresee the distinct role that diverse types of nonlinearity and asymmetry play in thermal conduction and rectification.

DOI: [10.1103/PhysRevE.104.014106](https://doi.org/10.1103/PhysRevE.104.014106)**I. INTRODUCTION**

Simplified microscopic models, such as classical particle chains in contact with heat baths, have proven useful to grasp the physics of thermal transport in low dimensions [1–4]. The interest in one-dimensional models goes beyond the theoretical challenge to derive the laws of heat conduction from the microscopic dynamics, insofar as they can be useful for understanding the anomalies observed in real systems, such as carbon nanotubes [5], nanowires [6], and molecular chains [7,8]. Moreover, these experiments and theories can lead to the development of new technologies for heat flow manipulation [9]. An interesting example is the thermal diode, whose thermal conductivity along a given axis changes depending on the direction of the heat flux, yielding rectification in a preferential direction. This proposal, initially conceived through simplified theoretical modeling [10], soon found materialization in solid-state experiments [11].

Subsequently, several variants of microscopic models were proposed to determine the conditions to achieve efficient rectification, by analyzing for instance, the effects of the range of the interactions or graded masses [12,13] and the role of the interface [14–18], among others. In the meantime, several efforts have been directed towards an analytical understanding of the diode effect, putting into evidence the requirements of asymmetry and nonlinearity for rectification, for instance, by linearizing the equations of motion but, as counterpart, making the parameters along a mass graded chain temperature dependent [19]. Closely related, in a very recent work, the diode effect was shown in the so-called temperature-gradient harmonic oscillator chains [20]. In the same spirit, a minimalistic model of two harmonic oscillators with temperature dependency has been recently studied [21]. The two-segment chain of classical spins in contact with multiple heat baths has also been studied [22], as well as quantum systems, to

show rectification of the heat flow between two thermal baths through a pair of interacting qubits [23] or even quantum spin chains [24].

Here we investigate a minimalist model of only two interacting classical particles connected to heat baths, in order to understand the diode effect directly from the equations of motion. We solve these equations in the limit of small nonlinearity, from a perturbative approach. Then we obtain expressions for the heat flow and rectification factor allowing us to directly grasp the impact of asymmetries and nonlinearities, as well as qualitative features of heat conduction and rectification, explicitly expressed in terms of the model parameters.

The paper is organized as follows. The system is defined in Sec. II. The perturbative solution and associated heat flow are described in Secs. III and IV, respectively, while the mathematical derivations can be found in the Appendix. The diode effect is discussed in Sec. V with final remarks in Sec. VI.

II. THE SYSTEM

We consider a one-dimensional system composed of two particles, with masses m_j (with $j = A, B$), coordinates x and y , subject to on-site potentials V_j and interacting through a potential V_I such that the complete Hamiltonian is

$$\mathcal{H} = \frac{p_A^2}{2m_A} + V_A(x) + \frac{p_B^2}{2m_B} + V_B(y) + V_I(x - y). \quad (1)$$

Moreover, each particle j is put in contact with a Langevin thermal bath at temperature T_j . A pictorial representation of this kind of system is provided in Fig. 1. Let us remark that this system is very similar to the couple of harmonic oscillators recently investigated [21], but in our case we introduce nonlinear forces. Namely, we treat the case where

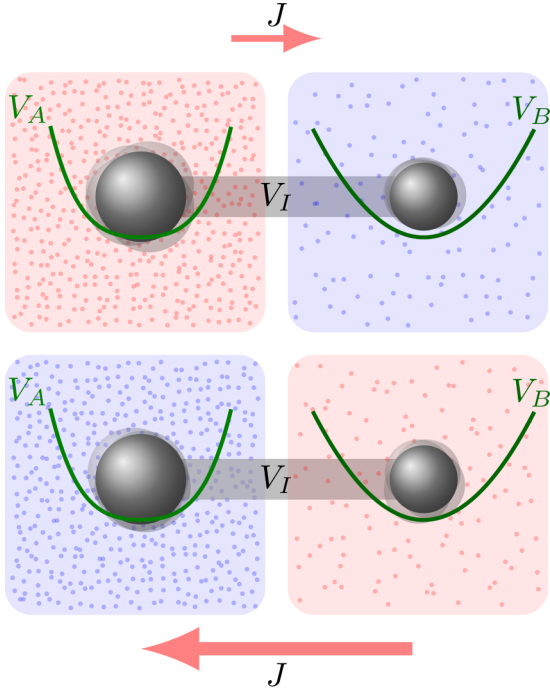


FIG. 1. Schematic representation of a minimalist thermal diode.

the interaction potential is harmonic with stiffness k_I , while the on-site potential of particle j is $V_j(z) = k_j z^2/2 + \epsilon V_j^{nl}(z)$, where k_j is the harmonic stiffness and $f_j(z) = -dV_j^{nl}(z)/dz$ is an arbitrary nonlinear force, whose intensity is controlled by the unitless constant ϵ . Explicitly, the equations of motion are

$$m_A \ddot{x} + \gamma_A \dot{x} + k_A x + k_I(x - y) = \epsilon f_A(x) + \eta_A(t), \quad (2)$$

$$m_B \ddot{y} + \gamma_B \dot{y} + k_B y + k_I(y - x) = \epsilon f_B(y) + \eta_B(t), \quad (3)$$

where ϵ is a dimensionless parameter that controls the strength of the nonlinear forces, γ_j is the damping coefficient, and η_j is the fluctuating force of the Langevin thermostat j ($j = A, B$), where η_A and η_B are independent zero-mean Gaussian-distributed white noises with

$$\langle \eta_A(t) \eta_A(t') \rangle = 2\gamma_A T_A \delta(t - t'),$$

$$\langle \eta_B(t) \eta_B(t') \rangle = 2\gamma_B T_B \delta(t - t'),$$

where the temperature is in units of the Boltzmann constant. Although we might suppress some parameters by fixing space and timescales, we will keep them explicit to preserve the AB symmetry of the equations.

III. PERTURBATIVE SOLUTION

Equations (2) and (3) cannot be solved exactly, however, if ϵ is small enough to ensure that the energy stored in the nonlinear mode is much smaller than in the harmonic one, we can expand the coordinates as

$$x(t) = x_0(t) + \epsilon x_1(t) + O(\epsilon^2), \quad (4)$$

$$y(t) = y_0(t) + \epsilon y_1(t) + O(\epsilon^2), \quad (5)$$

where the zeroth-order terms follow the equations

$$m_A \ddot{x}_0 + \gamma_A \dot{x}_0 + k_A x_0 + k_I(x_0 - y_0) = \eta_A(t), \quad (6)$$

$$m_B \ddot{y}_0 + \gamma_B \dot{y}_0 + k_B y_0 + k_I(y_0 - x_0) = \eta_B(t), \quad (7)$$

which are linear and uncoupled equations, and the first-order corrections x_1 and y_1 follow

$$m_A \ddot{x}_1 + \gamma_A \dot{x}_1 + k_A x_1 + k_I(x_1 - y_1) = f_A(x_0), \quad (8)$$

$$m_B \ddot{y}_1 + \gamma_B \dot{y}_1 + k_B y_1 + k_I(y_1 - x_1) = f_B(y_0). \quad (9)$$

Since we are interested in the long-time behavior, the initial conditions are not relevant; therefore we will use the Fourier transform, defined as $\tilde{z}(\omega) = \int_{-\infty}^{\infty} dt z(t) e^{-i\omega t}$, to solve the above stochastic differential equations. We start by expressing Eqs. (6) and (7) in Fourier space:

$$\underbrace{(k_A + k_I - m_A \omega^2 + i\gamma_A \omega)}_{a(\omega)} \tilde{x}_0 - k_I \tilde{y}_0 = \tilde{\eta}_A(\omega), \quad (10)$$

$$\underbrace{(k_B + k_I - m_B \omega^2 + i\gamma_B \omega)}_{b(\omega)} \tilde{y}_0 - k_I \tilde{x}_0 = \tilde{\eta}_B(\omega), \quad (11)$$

whose solution in matrix form is

$$\begin{pmatrix} \tilde{x}_0(\omega) \\ \tilde{y}_0(\omega) \end{pmatrix} = \begin{pmatrix} b(\omega) & k_I \\ k_I & a(\omega) \end{pmatrix}^{-1} \begin{pmatrix} \tilde{\eta}_A(\omega) \\ \tilde{\eta}_B(\omega) \end{pmatrix}. \quad (12)$$

Similarly, solving Eqs. (8) and (9) in Fourier space, we obtain (for more details see Ref. [1])

$$\begin{pmatrix} \tilde{x}_1(\omega) \\ \tilde{y}_1(\omega) \end{pmatrix} = \begin{pmatrix} b(\omega) & k_I \\ k_I & a(\omega) \end{pmatrix}^{-1} \begin{pmatrix} \mathcal{F}\{f_A(x_0)\}(\omega) \\ \mathcal{F}\{f_B(y_0)\}(\omega) \end{pmatrix}. \quad (13)$$

IV. HEAT FLOW

The heat flow J along the system can be defined in several forms that are equivalent when the system reaches a stationary state (see, for instance, Ref. [3]). The potential $V_I(x - y)$ represents the energy stored in the interaction between neighboring particles, and the energetic flow can be written as

$$\frac{d}{dt} \langle V_I(x - y) \rangle = \langle V_I'(x - y) \dot{x} \rangle - \langle V_I'(x - y) \dot{y} \rangle,$$

and, under stationarity, $\langle V_I'(x - y) \dot{x} \rangle = \langle V_I'(x - y) \dot{y} \rangle$. From this identity, we have equivalent definitions that in our case, where $V_I'(x - y) = k_I(x - y)$, read

$$J = \langle k_I(x - y) \dot{x} \rangle = \langle k_I(x - y) \dot{y} \rangle, \quad (14)$$

or still $J = \langle k_I(x - y)(\dot{x} + \dot{y})/2 \rangle$. The heat flow J can also be expanded in a series of ϵ , as

$$J = J_0 + \epsilon J_1 + O(\epsilon^2). \quad (15)$$

In the linear regime, Eq. (14) yields (see Appendix A 2)

$$J_0 = k_I \langle x_0 \dot{x}_0 \rangle - k_I \langle y_0 \dot{x}_0 \rangle \quad (16)$$

$$= -k_I \int \frac{d\omega d\omega'}{(2\pi)^2} e^{i\omega(\omega+\omega')} \langle \tilde{y}_0(\omega) i\omega' \tilde{x}_0(\omega') \rangle. \quad (17)$$

Then, we obtain

$$J_0 = \kappa_0 [T_A - T_B], \quad (18)$$

TABLE I. Nonlinear force f_j and associated function g_j (derived in Appendix A 2).

$f_j(z) = \sum_{n \geq 0} c_{j,n} z^n$	$g_j(z) = \sum_{n \geq 1} c_{j,n} n!! z^{(n-1)/2}$
$-z^{2n-1}, n \in \mathbb{N}$	$-(2n-1)!! z^{n-1}$
$-\sin(Kz)$	$-Ke^{-K^2 z/2}$
$-\sinh(Kz)$	$-Ke^{K^2 z/2}$

where the zeroth-order thermal conductivity is

$$\kappa_0 = \int \frac{d\omega}{2\pi} \frac{2\gamma^2 k_l^2 \omega^2}{|a(\omega)b(\omega) - k_l^2|^2}. \quad (19)$$

Note that this expression shows that, regardless of the asymmetries that may be present, the linear system cannot be converted to a thermal diode since κ_0 does not depend on the temperatures and it is invariant under particle exchange; hence, the magnitude of the flow is the same in both directions.

With regard to the dependence of κ_0 on the coupling strength k_l , Eq. (19) gives $\kappa_0 \sim k_l^2 + O(k_l^3)$, for small k_l . It is interesting to note that this is the scaling observed for two-segment chains with nonlinear forces of Frenkel-Kontorova (FK) type [10].

Now we proceed to calculate the first-order correction of the current J , containing the information on the nonlinearities. From Eq. (14), we have

$$\begin{aligned} J &= -k_l \langle y(t) \dot{x}(t) \rangle \\ &= \underbrace{-k_l \langle y_0 \dot{x}_0 \rangle}_{J_0} + \epsilon \underbrace{(-k_l) [\langle y_1 \dot{x}_0 \rangle + \langle y_0 \dot{x}_1 \rangle]}_{J_1}, \end{aligned} \quad (20)$$

where the correlations in J_1 are calculated in Appendix A 2, yielding $J_1 = \kappa_1(T_A, T_B) \Delta T$, with

$$\kappa_1(T_A, T_B) = \kappa_0 \sum_{j=A,B} \beta_j g_j(\sigma_{mj} T_m + \sigma_j T_j), \quad (21)$$

where $T_m = (T_A + T_B)/2$ is the mean temperature, β_j, σ_{mj} and σ_j ($j = A, B$) are coefficients that do not depend on the temperature (derived in Appendix A 2, where explicit expressions are also given), and g_j is derived from the Fourier transform of the force f_j (for examples see Table I).

In Fig. 2 an illustrative example shows the good agreement between the first-order theoretical prediction, Eq. (20), and the numerical evaluation of Eq. (14), performed over trajectories obtained from the numerical integration of the equations of motion, using an eighth-order Runge-Kutta algorithm [25].

For weak coupling, the scaling

$$\kappa \sim k_l^2 + O(k_l^3, \epsilon k_l^2), \quad (22)$$

obtained in the linear case, still holds, while κ tends to a constant value for large k_l . Of course, if the interfacial interaction, which connects the two units of the system, vanishes, hence, κ vanishes too, as expected due to disruption of the channel for energy flux.

As a check of consistency, we verified that, if $f_j(z)$ were linear, then $g_j(z)$ would be a constant $\bar{g}_j < 0$ ($n = 0$ in Table I), in which case Eq. (21) becomes $\kappa_1 = (\beta_A \bar{g}_A + \beta_B \bar{g}_B) \kappa_0$ in accord with the zeroth-order expression for

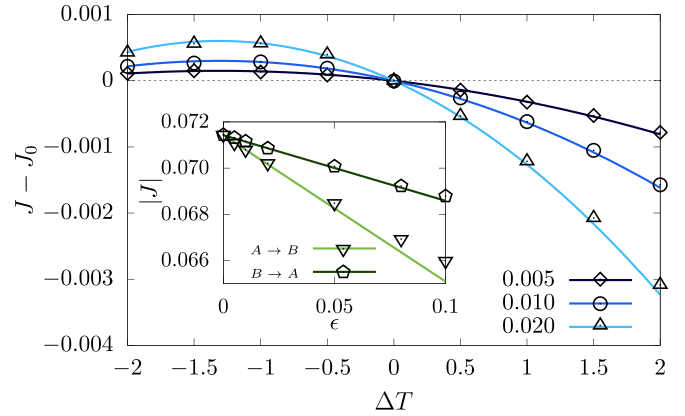


FIG. 2. Heat current difference $J - J_0$ vs ΔT . Solid lines correspond to the theoretical prediction given by Eq. (20) and symbols to the computation from numerical integration of the equations of motion, averaged over 10^5 realizations. $V_A^{nl}(z) = z^4/4$, $V_B^{nl}(z) = 0$. Different values of ϵ indicated on the figure were considered, $k_l = 0.5$, and all other parameters are equal to 1. The inset shows the current $|J|$ as a function of ϵ for $\Delta T = \pm 1$ (i.e., $A \rightleftharpoons B$).

κ_0 , Eq. (19), after substituting $k_A \rightarrow k_A - \epsilon \bar{g}_A$ and $k_B \rightarrow k_B - \epsilon \bar{g}_B$.

Since the linear conductivity κ_0 does not depend on the bath temperatures, the heat flux will have the same magnitude in both directions. Therefore, for rectification, it is crucial that at least one of the two forces $f_j(z)$ be nonlinear. This nonlinearity would act by introducing a dependence of the conductivity on the temperatures, through the argument of $g_j(z)$ in Eq. (21), which originates from the correlations of the zeroth-order coordinates. A temperature dependence that is asymmetric under particle exchange is then responsible for thermal rectification, as discussed in the next section. Moreover, this is the basis of the diode effect on harmonic systems with imposed or natural temperature dependencies [19–21].

V. DIODE EFFECT

First, recall that β_j, σ_{mj} , and σ_j , which define J_1 , are quantities that do not depend on the end temperatures. While σ_{mj} (as well as κ_0) is always positive, β_j and σ_j do not have a definite sign in general; however, $\sigma_{mj} T_m + \sigma_j T_j$ must be positive. Moreover, in contrast to κ_0 and σ_{mj} , whose expressions are invariant by AB exchange, the coefficients β_j or σ_j may be nonsymmetric in general, which would ensure that even if $g_A = g_B$, the conductivity can become dependent on the direction of the flux.

Let us define the fluxes J_{AB} and J_{BA} for the positive temperature gradient ($T_A = T_h > T_c = T_B$) and the reversed one, as schematized in Fig. 1. From the expression of J , we have

$$\begin{aligned} J_{AB} &\equiv J_{A \rightarrow B} = [\kappa_0 + \epsilon \underbrace{\kappa_1(T_h, T_c)}_{\kappa_1^{AB}}] (T_h - T_c), \\ J_{BA} &\equiv J_{B \rightarrow A} = [\kappa_0 + \epsilon \underbrace{\kappa_1(T_c, T_h)}_{\kappa_1^{BA}}] (T_c - T_h). \end{aligned} \quad (23)$$

Rectification emerges when $\kappa_1^{AB} \neq \kappa_1^{BA}$, molded by the functions $g_j(z)$, associated to nonlinear forces $f_j(z)$, which introduce the dependence of the conductivity on the bath temperatures.

In what follows, to quantify the diode effect, we use the ratio

$$\chi \equiv \frac{||J_{AB}| - |J_{BA}||}{[|J_{AB}| + |J_{BA}|]/2} = \epsilon \frac{|\kappa_1^{AB} - \kappa_1^{BA}|}{\kappa_0} + O(\epsilon^2). \quad (24)$$

This quantity coincides with the rectification factor [10] at first order in ϵ , and it is twice the diodicity [26]. Notice that the departure from the linear regime, signaled by $\epsilon \neq 0$, together with asymmetry, is required to allow the diode effect ($\chi \neq 0$) at first order in ϵ . However, the rectification χ is small, of order ϵ .

In the following sections, we will discuss the behavior of χ in some particular cases, in order to reduce the number of parameters.

A. Symmetric chain

Let us address the case where $k_A = k_B$, $m_A = m_B$ and $\gamma_A = \gamma_B$, hence, the asymmetry required for rectification must reside in the nonlinear on-site forces. In this simple case, the coefficients obtained in Appendix A 2 reduce to

$$\sigma_m = \frac{[(k + k_I)\bar{m} + 1]k_I^2}{k(k + 2k_I)(k + k_I + \bar{m}k_I^2)}, \quad (25)$$

$$\sigma_A = \sigma_B = \sigma = \frac{1}{k + k_I + \bar{m}k_I^2}, \quad (26)$$

$$\beta_A = \beta_B = \sigma/2. \quad (27)$$

Then

$$\chi = \epsilon \frac{|g_A(T_+) - g_A(T_-) + g_B(T_-) - g_B(T_+)|}{2(k + k_I + \bar{m}k_I^2)}, \quad (28)$$

where $T_{\pm} = \sigma_m T_m + \sigma T_h = (\sigma_m + \sigma)T_m \pm \sigma(T_h - T_c)/2$.

First, we notice that χ is finite in the limit $k_I \rightarrow 0$, and it tends to zero in the opposite limit $k_I \rightarrow \infty$. Examples are given in Fig. 3 for two different potentials.

Rectification enhancement can be achieved by augmenting the temperature difference, fixing the average, since $\Delta g_j \equiv g_j(T^+) - g_j(T^-) \approx g'_j((\sigma_m + \sigma)T_m) \Delta T + O((\Delta T)^3)$. This effect is illustrated in Fig. 4. As a matter of fact, the increase of the rectification factor with the temperature difference has been observed in diverse models [13,16,27].

The mass and inverse square damping contribute trough $\bar{m} = m/\gamma^2$ to spoil rectification if $k_I > 0$. This suggests that the overdamped regime would perform rectification better.

We can also understand how the preferential direction in which the conductivity is larger, for given bath temperatures, depends on the type of nonlinear forces. For instance, let us consider $g_B(z) = 0$. If $g_A(z)$ is monotonically decreasing, like in the power-law case of Table I, then $\Delta g_A < 0$, for $T_A > T_B$, indicating that the preferential direction is from B to A (in general from smaller to larger nonlinear force). However, if the potential is sinusoidal, $g_A(z)$ is an increasing function (Table I), then the preferential direction is inverted with respect to the previous case (i.e., it is from A to B), as observed for asymmetric FK chains [10].

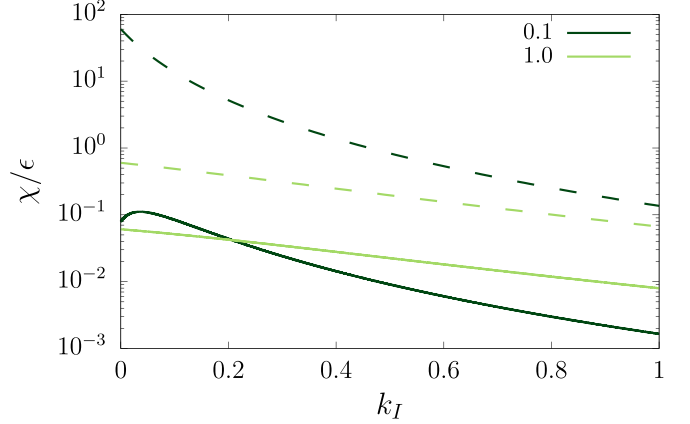


FIG. 3. Scaled rectification factor as a function of the interfacial stiffness k_I , for the nonlinear on-site potential $V_A^{nl}(z) = z^4/4$, (power law, dashed lines), and $V_A^{nl}(z) = -\cos(z)$, (sinusoidal, solid lines), for $k = 0.1$ (dark green) and 1 (light green), as indicated in the legend. In all cases $V_B^{nl} \equiv 0$, $\bar{m} = 1$, $T_m = 1$, $\Delta T = 0.4$.

Let us take a closer look to the conductivity in the limit $k_I \rightarrow 0$, for some concrete potentials V_A^{nl} , while $V_B^{nl} = 0$. Recall that the conductivity scales with k_I^2 , then the fluxes vanish in the limit $k_I \rightarrow 0$; however, χ can be large for finite but very small k_I . In that limit, we have $\sigma_m = 0$, $\sigma = 1/k$, hence the scaled mass \bar{m} does not play a role in the rectification.

For the power-law on-site potential $V_A^{nl}(z) = z^{2n}/(2n)$, $g_A(z) = -(2n-1)!!z^{n-1}$, with $n > 1$, in the limit $k_I \rightarrow 0$, Eq. (28) becomes

$$\chi = \epsilon \frac{(2n-1)!!}{2k} \left[\left(\frac{T_h}{k} \right)^{n-1} - \left(\frac{T_c}{k} \right)^{n-1} \right]. \quad (29)$$

Equation (29) predicts, for instance, that the ratio χ grows with the temperature difference $\Delta T = T_h - T_c$, with positive

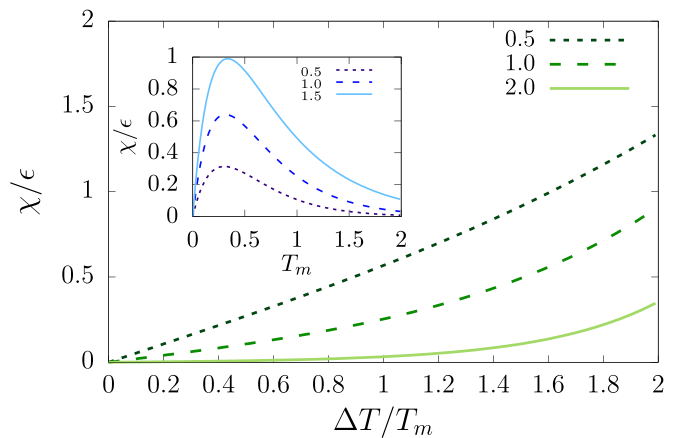


FIG. 4. Scaled rectification factor as a function of the relative temperature difference $\Delta T/T_m$, for the nonlinear on-site potential $V_A^{nl}(z) = -\cos(z)$, $V_B^{nl} \equiv 0$, $k = k_I = 0.1$, for different values of T_m , indicated in the legend. The inset displays the scaled rectification vs T_m for different values of ΔT indicated in the legend, showing that there is an optimal T_m , due to the loss of nonlinearity in the extremes of low and high temperatures for the chosen potential.

concavity for $n > 2$, nearly linear for small ΔT . These effects persist for finite k_l as shown in Fig. 4.

For the sinusoidal on-site potential $V_A^{nl}(z) = -\cos(Kz)/K$ (as in the FK model), $g_A(z) = -Ke^{-K^2z/2}$ (see Table I). In this case the dependence χ versus k_l can be nonmonotonic, with a finite optimal value, as shown in Fig. 3. In the limit $k_l \rightarrow 0$ we obtain

$$\chi = \epsilon \frac{K}{2k} (e^{-K^2T_c/(2k)} - e^{-K^2T_h/(2k)}). \quad (30)$$

The dependence on ΔT (for fixed mean temperature T_m) is also an increasing convex function. This behavior, which also holds for finite k_l , as exemplified in Fig. 4, is qualitatively similar to that reported from simulations of diode models [13,16,27]. For the power-law potential the nonlinear correction is weak but in the same direction.

B. Small k_l limit

In the previous section, we have seen that the limit of small k_l is relevant, while it allows to simplify the analytical expressions significantly. Then, in this limit, we will analyze the effect of introducing the asymmetry alternatively in the stiffness ($k_A \neq k_B$), mass ($m_A \neq m_B$), or damping coefficient ($\gamma_A \neq \gamma_B$). As shown in Appendix A 3, in this limit,

$$\kappa_1 \simeq \kappa_0 [\beta_A g_A(\sigma_A T_A) + \beta_B g_B(\sigma_B T_B)], \quad (31)$$

where the explicit expressions for the coefficients are given in the Appendix A 3 for each asymmetry. The results for the rectification factor χ are illustrated in Fig. 5.

Note that we observe that any of these asymmetries can produce rectification. In particular, notice that, even when the chain is homogeneous, distinct thermostats (characterized by different friction coefficients) can also produce a diode effect.

VI. FINAL REMARKS

We have presented analytical results starting from the microscopic classical dynamics of a two-particle system with nonlinear forces. Due to the nonlinearity of the equations, we tackled the solution from a perturbative approach valid for small nonlinear intensity ϵ . It is noticeable that despite the simplicity of the system, the conductivity $\kappa = \kappa_0 + \epsilon\kappa_1$ has an intricate dependence on the system parameters. Therefore, it might be hard to make a portrait of this complexity only through molecular dynamics simulations, making valuable the present effort of obtaining analytical results from first principles.

Some previously known results can be revisited from this perspective. Particularly, one can see how the temperature dependence of the conductivity emerges from the nonlinearity of the forces, through the functions $g_j(z)$. The requirements of broken symmetry and of nonlinearity explicitly appear. The results also allow shedding light on effects observed in chains, e.g., the scaling of the conductivity with the interfacial stiffness k_l , the dependence of the rectification factor on k_l and on the temperature difference. How nonlinearities determine the preferential direction has also been foreseen. The role of

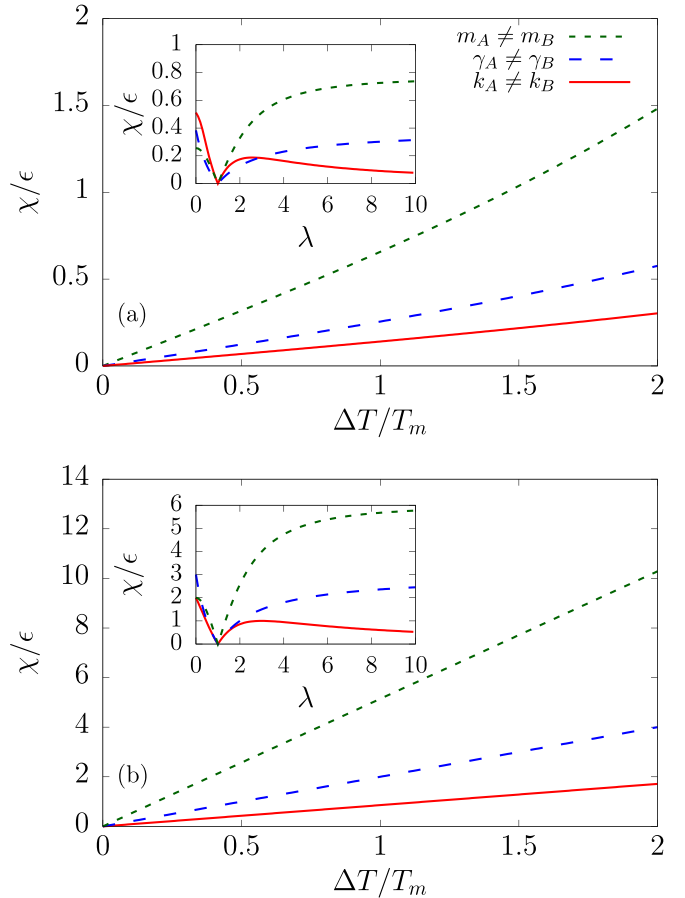


FIG. 5. Scaled rectification factor vs the relative temperature difference $\Delta T/T_m$, with $T_m = 1$, for nonlinear on-site potential $V_A^{nl}(z) = V_B^{nl}(z) =$ (a) $-\cos(z)$ and (b) $z^4/4$ for $m_A = 5$, $k_A = k_B = m_B = \gamma_A = \gamma_B = 1$ (green), $\gamma_A = 5$, $\gamma_B = k_A = k_B = m_A = m_B = 1$ (blue) $k_A = 5$, $k_B = m_A = m_B = \gamma_A = \gamma_B = 1$ (red). The insets show the dependence on the asymmetry factor λ that for each parameter p gives $p_A = \lambda p_B = \lambda$.

different asymmetries (in the mass, stiffness, on-site potential and even damping coefficient) was also shown.

It is interesting to note that, from Appendix A 2, it is possible to obtain that the nonlinearity yields a temperature-dependent power spectrum (anharmonic phonons), which can be seen as the correction to the harmonic theory responsible for phonon scattering [28]. The relationship between temperature and the overlapping phonon bands has already been analytically studied for FK asymmetric chains [10] and chains with dissimilar anharmonic segments (FK and Fermi-Pasta-Ulan-Tsingou) [10,17].

Our results are valid when the effect of the nonlinear forces can be treated as a perturbation to the predominantly linear solutions. Consequently, the predicted diode effect is very small. However, the results allow for a clear glance regarding the mechanisms behind rectification and the role of diverse asymmetries and nonlinearities.

Possible extensions include baths of different nature (correlated or non-Gaussian) and nonlinear interfacial interactions.

ACKNOWLEDGMENTS

We are grateful to Alexandre Almeida for fruitful discussions. C.A. acknowledges Brazilian agency CNPq (process 311435/2020-3) for partial financial support. This study was financed in part by the Coordenação de Aperfeiçoamento de Pessoal de Nível Superior - Brasil (CAPES) - Finance Code 001.

APPENDIX

1. Perturbative solution

a. Zeroth order

Equations (10) and (11) in matrix form are

$$\begin{pmatrix} a(\omega) & -k_I \\ -k_I & b(\omega) \end{pmatrix} \begin{pmatrix} \tilde{x}_0(\omega) \\ \tilde{y}_0(\omega) \end{pmatrix} = \begin{pmatrix} \tilde{\eta}_A(\omega) \\ \tilde{\eta}_B(\omega) \end{pmatrix}, \quad (\text{A1})$$

whose solution, by matrix inversion, is

$$\begin{pmatrix} \tilde{x}_0(\omega) \\ \tilde{y}_0(\omega) \end{pmatrix} = \frac{1}{a(\omega)b(\omega) - k_I^2} \begin{pmatrix} b(\omega) & k_I \\ k_I & a(\omega) \end{pmatrix} \begin{pmatrix} \tilde{\eta}_A(\omega) \\ \tilde{\eta}_B(\omega) \end{pmatrix} = \begin{pmatrix} M_{11}(\omega) & M_{12}(\omega) \\ M_{21}(\omega) & M_{22}(\omega) \end{pmatrix} \begin{pmatrix} \tilde{\eta}_A(\omega) \\ \tilde{\eta}_B(\omega) \end{pmatrix}, \quad (\text{A2})$$

corresponding to Eq. (12). The Fourier transforms $\tilde{\eta}_A(\omega)$ and $\tilde{\eta}_B(\omega)$ are also Gaussian distributed with

$$\langle \tilde{\eta}_A(\omega) \rangle = \langle \tilde{\eta}_B(\omega) \rangle = 0, \quad (\text{A3})$$

$$\langle \tilde{\eta}_A(\omega) \tilde{\eta}_A(\omega') \rangle = 2\gamma T_A [2\pi \delta(\omega + \omega')], \quad (\text{A4})$$

$$\langle \tilde{\eta}_B(\omega) \tilde{\eta}_B(\omega') \rangle = 2\gamma T_B [2\pi \delta(\omega + \omega')]. \quad (\text{A5})$$

Using the solutions and the correlations of the noises, we can calculate the coordinate correlations in Fourier space:

$$\langle \tilde{x}_0(\omega) \tilde{x}_0(\omega') \rangle = 2\gamma [M_{11}(\omega)M_{11}(\omega')T_A + M_{12}(\omega)M_{12}(\omega')T_B] 2\pi \delta(\omega + \omega'), \quad (\text{A6})$$

$$\langle \tilde{y}_0(\omega) \tilde{y}_0(\omega') \rangle = 2\gamma [M_{21}(\omega)M_{21}(\omega')T_A + M_{22}(\omega)M_{22}(\omega')T_B] 2\pi \delta(\omega + \omega'), \quad (\text{A7})$$

$$\langle \tilde{x}_0(\omega) \tilde{y}_0(\omega') \rangle = 2\gamma [M_{11}(\omega)M_{21}(\omega')T_A + M_{12}(\omega)M_{22}(\omega')T_B] 2\pi \delta(\omega + \omega'). \quad (\text{A8})$$

b. First order

The Fourier-transformed Eqs. (8) and (9) in matrix form are

$$\begin{pmatrix} a(\omega) & -k_I \\ -k_I & b(\omega) \end{pmatrix} \begin{pmatrix} \tilde{x}_1(\omega) \\ \tilde{y}_1(\omega) \end{pmatrix} = \begin{pmatrix} \mathcal{F}\{f_A(x_0)\}(\omega) \\ \mathcal{F}\{f_B(y_0)\}(\omega) \end{pmatrix}, \quad (\text{A9})$$

and their respective solutions are

$$\begin{pmatrix} \tilde{x}_1(\omega) \\ \tilde{y}_1(\omega) \end{pmatrix} = \begin{pmatrix} M_{11}(\omega) & M_{12}(\omega) \\ M_{21}(\omega) & M_{22}(\omega) \end{pmatrix} \begin{pmatrix} \mathcal{F}\{f_A(x_0)\}(\omega) \\ \mathcal{F}\{f_B(y_0)\}(\omega) \end{pmatrix}, \quad (\text{A10})$$

giving Eq. (13). Recalling that $f_i(z) = \sum_n c_{i,n} z^n$, for $i = A, B$, then

$$\mathcal{F}\{f_i(z)\} = \sum_n c_{i,n} \mathcal{F}\{z^n\}(\omega), \quad (\text{A11})$$

leading to

$$\begin{aligned} \tilde{x}_1(\omega) &= M_{11}(\omega) \mathcal{F}\{f_A(x_0)\}(\omega) + M_{12}(\omega) \mathcal{F}\{f_B(y_0)\}(\omega) \\ &= M_{11}(\omega) \sum_n c_{A,n} \mathcal{F}\{x_0^n\}(\omega) + M_{12}(\omega) \sum_n c_{B,n} \mathcal{F}\{y_0^n\}(\omega), \end{aligned} \quad (\text{A12})$$

$$\begin{aligned} \tilde{y}_1(\omega) &= M_{21}(\omega) \mathcal{F}\{f_A(x_0)\}(\omega) + M_{22}(\omega) \mathcal{F}\{f_B(y_0)\}(\omega) \\ &= M_{21}(\omega) \sum_n c_{A,n} \mathcal{F}\{x_0^n\}(\omega) + M_{22}(\omega) \sum_n c_{B,n} \mathcal{F}\{y_0^n\}(\omega). \end{aligned} \quad (\text{A13})$$

Moreover, we will use below that the Fourier transform of an integer power of a function $z(t)$ is

$$\mathcal{F}\{z^n\}(\omega) = \int \prod_{j=1}^n \frac{d\omega_j}{2\pi} \delta\left(\omega - \sum_{j=1}^n \omega_j\right) \prod_{j=1}^n \tilde{z}(\omega_j). \quad (\text{A14})$$

2. Heat flow

a. Zeroth order

From Eq. (14), using the first definition and writing the average in Fourier space

$$J_x = k_I \langle (x_0 - y_0) \dot{x}_0 \rangle = k_I \int \frac{d\omega d\omega'}{(2\pi)^2} e^{it(\omega+\omega')} \langle [\tilde{x}_0(\omega) - \tilde{y}_0(\omega)] [i\omega' \tilde{x}_0(\omega')] \rangle, \quad (\text{A15})$$

the first term is null since $\langle \tilde{x}_0(\omega) \tilde{x}_0(-\omega) \rangle$ is an even function, when we multiply times $i\omega$ from the time derivative, the function becomes odd, and as we integrate for all ω , the value becomes null. Then, using Eq. (A8),

$$\begin{aligned} J_0 = J_x &= -k_I \int \frac{d\omega}{2\pi} e^{it(\omega+\omega')} (i\omega') \langle \tilde{y}_0(\omega) \tilde{x}_0(\omega') \rangle \\ &= k_I \int \frac{d\omega}{2\pi} 2\gamma(i\omega) \left\{ \frac{k_I b(-\omega) T_A + k_I a(\omega) T_B}{[a(\omega)b(\omega) - k_I^2][a(-\omega)b(-\omega) - k_I^2]} \right\}, \end{aligned} \quad (\text{A16})$$

which, if we perform a change of variables ($\omega \rightarrow -\omega$) in the second term gives

$$J_0 = k_I \int \frac{d\omega}{2\pi} 2\gamma(i\omega) \left\{ \frac{k_I b(-\omega) T_A - k_I a(-\omega) T_B}{[a(\omega)b(\omega) - k_I^2][a(-\omega)b(-\omega) - k_I^2]} \right\}, \quad (\text{A17})$$

where only the odd parcel of the numerator (since the denominator is always even) will yield a non-null result after the integration. We expand the expression to

$$J_0 = \int \frac{d\omega}{2\pi} \left\{ \frac{2\gamma^2 k_I^2 \omega^2}{[a(\omega)b(\omega) - k_I^2][a(-\omega)b(-\omega) - k_I^2]} \right\} (T_A - T_B) \equiv \kappa_0 (T_A - T_B), \quad (\text{A18})$$

corresponding to Eqs. (16) and (19).

b. First order

The correlations required to compute J_1 are

$$\begin{aligned} \langle y_1 \dot{x}_0 \rangle &= \int \frac{d\omega d\omega'}{(2\pi)^2} e^{it(\omega+\omega')} (i\omega') \langle \tilde{y}_1(\omega) \tilde{x}_0(\omega') \rangle \\ &= \int \frac{d\omega d\omega'}{(2\pi)^2} e^{it(\omega+\omega')} (i\omega') \sum_n [c_{A,n} M_{21}(\omega) \langle \mathcal{F}\{x_0^n\}(\omega) \tilde{x}_0(\omega') \rangle + c_{B,n} M_{22}(\omega) \langle \mathcal{F}\{y_0^n\}(\omega) \tilde{x}_0(\omega') \rangle], \end{aligned} \quad (\text{A19})$$

and

$$\begin{aligned} \langle y_0 \dot{x}_1 \rangle &= \int \frac{d\omega d\omega'}{(2\pi)^2} e^{it(\omega+\omega')} (i\omega') \langle \tilde{y}_0(\omega) \tilde{x}_1(\omega') \rangle \\ &= \int \frac{d\omega d\omega'}{(2\pi)^2} e^{it(\omega+\omega')} (i\omega') \sum_n [c_{A,n} M_{11}(\omega') \langle \mathcal{F}\{x_0^n\}(\omega') \tilde{y}_0(\omega) \rangle + c_{B,n} M_{12}(\omega') \langle \mathcal{F}\{y_0^n\}(\omega') \tilde{y}_0(\omega) \rangle]. \end{aligned} \quad (\text{A20})$$

First, we evaluate the following correlations between the zeroth-order terms,

$$\begin{aligned} \int \frac{d\omega_1 d\omega_2}{(2\pi)^2} \langle \tilde{x}_0(\omega_1) \tilde{x}_0(\omega_2) \rangle &= 2\gamma \int \frac{d\omega}{2\pi} [M_{11}(\omega) M_{11}(-\omega) T_A + M_{12}(\omega) M_{12}(-\omega) T_B] \\ &= \sigma_{mA} T_m + \sigma_A T_A, \end{aligned} \quad (\text{A21})$$

$$\begin{aligned} \int \frac{d\omega_1 d\omega_2}{(2\pi)^2} \langle \tilde{y}_0(\omega_1) \tilde{y}_0(\omega_2) \rangle &= 2\gamma \int \frac{d\omega}{2\pi} [M_{21}(\omega) M_{21}(-\omega) T_A + M_{22}(\omega) M_{22}(-\omega) T_B] \\ &= \sigma_{mB} T_m + \sigma_B T_B. \end{aligned} \quad (\text{A22})$$

These correlations, together with Eq. (A14), will be used to evaluate the correlations required to compute J_1 :

$$\begin{aligned}
\langle \mathcal{F}(x_0^n)(\omega) \tilde{x}_0(\omega') \rangle &= \int \left(\prod_{j=1}^n \frac{d\omega_j}{2\pi} \right) \delta \left(\omega - \sum_{j=1}^n \omega_j \right) \left\langle \left[\prod_{j=1}^n \tilde{x}_0(\omega_j) \right] \tilde{x}_0(\omega') \right\rangle \\
&= n!! \int \left(\prod_{j=1}^n \frac{d\omega_j}{2\pi} \right) \delta \left(\omega - \sum_{j=1}^n \omega_j \right) \langle \tilde{x}_0(\omega_n) \tilde{x}_0(\omega') \rangle \prod_{j \text{ odd}}^{n-1} \langle \tilde{x}_0(\omega_j) \tilde{x}_0(\omega_{j+1}) \rangle \\
&= n!! 2\pi \delta(\omega + \omega') \int \frac{d\omega_n}{2\pi} \langle \tilde{x}_0(\omega_n) \tilde{x}_0(\omega') \rangle \prod_{j \text{ odd}}^{n-1} \int \frac{d\omega_j d\omega_{j+1}}{(2\pi)^2} \langle \tilde{x}_0(\omega_j) \tilde{x}_0(\omega_{j+1}) \rangle \\
&= n!! 2\pi \delta(\omega + \omega') \int \frac{d\omega_n}{2\pi} \langle \tilde{x}_0(\omega_n) \tilde{x}_0(\omega') \rangle (\sigma_{m_A} T_m + \sigma_A T_A)^{\frac{n-1}{2}}, \tag{A23}
\end{aligned}$$

$$\begin{aligned}
\langle \mathcal{F}(x_0^n)(\omega) \tilde{y}_0(\omega') \rangle &= \int \left(\prod_{j=1}^n \frac{d\omega_j}{2\pi} \right) \delta \left(\omega - \sum_{j=1}^n \omega_j \right) \left\langle \left[\prod_{j=1}^n \tilde{x}_0(\omega_j) \right] \tilde{y}_0(\omega') \right\rangle \\
&= n!! \int \left(\prod_{j=1}^n \frac{d\omega_j}{2\pi} \right) \delta \left(\omega - \sum_{j=1}^n \omega_j \right) \langle \tilde{x}_0(\omega_n) \tilde{y}_0(\omega') \rangle \prod_{j \text{ odd}}^{n-1} \langle \tilde{x}_0(\omega_j) \tilde{x}_0(\omega_{j+1}) \rangle \\
&= n!! 2\pi \delta(\omega + \omega') \int \frac{d\omega_n}{2\pi} \langle \tilde{x}_0(\omega_n) \tilde{y}_0(\omega') \rangle \prod_{j \text{ odd}}^{n-1} \int \frac{d\omega_j d\omega_{j+1}}{(2\pi)^2} \langle \tilde{x}_0(\omega_j) \tilde{x}_0(\omega_{j+1}) \rangle \\
&= n!! 2\pi \delta(\omega + \omega') \int \frac{d\omega_n}{2\pi} \langle \tilde{x}_0(\omega_n) \tilde{y}_0(\omega') \rangle (\sigma_{m_A} T_m + \sigma_A T_A)^{\frac{n-1}{2}}, \tag{A24}
\end{aligned}$$

$$\begin{aligned}
\langle \mathcal{F}(y_0^n)(\omega) \tilde{x}_0(\omega') \rangle &= \int \left(\prod_{j=1}^n \frac{d\omega_j}{2\pi} \right) \delta \left(\omega - \sum_{j=1}^n \omega_j \right) \left\langle \left[\prod_{j=1}^n \tilde{y}_0(\omega_j) \right] \tilde{x}_0(\omega') \right\rangle \\
&= n!! \int \left(\prod_{j=1}^n \frac{d\omega_j}{2\pi} \right) \delta \left(\omega - \sum_{j=1}^n \omega_j \right) \langle \tilde{y}_0(\omega_n) \tilde{x}_0(\omega') \rangle \prod_{j \text{ odd}}^{n-1} \langle \tilde{y}_0(\omega_j) \tilde{y}_0(\omega_{j+1}) \rangle \\
&= n!! 2\pi \delta(\omega + \omega') \int \frac{d\omega_n}{2\pi} \langle \tilde{y}_0(\omega_n) \tilde{x}_0(\omega') \rangle \prod_{j \text{ odd}}^{n-1} \int \frac{d\omega_j d\omega_{j+1}}{(2\pi)^2} \langle \tilde{y}_0(\omega_j) \tilde{y}_0(\omega_{j+1}) \rangle \\
&= n!! 2\pi \delta(\omega + \omega') \int \frac{d\omega_n}{2\pi} \langle \tilde{y}_0(\omega_n) \tilde{x}_0(\omega') \rangle (\sigma_{m_B} T_m + \sigma_B T_B)^{\frac{n-1}{2}}, \tag{A25}
\end{aligned}$$

$$\begin{aligned}
\langle \mathcal{F}(y_0^n)(\omega) \tilde{y}_0(\omega') \rangle &= \int \left(\prod_{j=1}^n \frac{d\omega_j}{2\pi} \right) \delta \left(\omega - \sum_{j=1}^n \omega_j \right) \left\langle \left[\prod_{j=1}^n \tilde{y}_0(\omega_j) \right] \tilde{y}_0(\omega') \right\rangle \\
&= n!! \int \left(\prod_{j=1}^n \frac{d\omega_j}{2\pi} \right) \delta \left(\omega - \sum_{j=1}^n \omega_j \right) \langle \tilde{y}_0(\omega_n) \tilde{y}_0(\omega') \rangle \prod_{j \text{ odd}}^{n-1} \langle \tilde{y}_0(\omega_j) \tilde{y}_0(\omega_{j+1}) \rangle \\
&= n!! 2\pi \delta(\omega + \omega') \int \frac{d\omega_n}{2\pi} \langle \tilde{y}_0(\omega_n) \tilde{y}_0(\omega') \rangle \prod_{j \text{ odd}}^{n-1} \int \frac{d\omega_j d\omega_{j+1}}{(2\pi)^2} \langle \tilde{y}_0(\omega_j) \tilde{y}_0(\omega_{j+1}) \rangle \\
&= n!! 2\pi \delta(\omega + \omega') \int \frac{d\omega_n}{2\pi} \langle \tilde{y}_0(\omega_n) \tilde{y}_0(\omega') \rangle (\sigma_{m_B} T_m + \sigma_B T_B)^{\frac{n-1}{2}}. \tag{A26}
\end{aligned}$$

Now we write Eq. (20) as

$$\begin{aligned}
-k_I \{ \langle y_1 \dot{x}_0 \rangle + \langle y_0 \dot{x}_1 \rangle \} &= -k_I \int \frac{d\omega d\omega'}{(2\pi)^2} e^{i\omega(\omega+\omega')} (i\omega') \sum_n \{ c_{A,n} [M_{21}(\omega) \langle \mathcal{F}\{x_0^n\}(\omega) \tilde{x}_0(\omega') \rangle + M_{11}(\omega') \langle \mathcal{F}\{x_0^n\}(\omega') \tilde{y}_0(\omega) \rangle] \\
&\quad + c_{B,n} [M_{22}(\omega) \langle \mathcal{F}\{y_0^n\}(\omega) \tilde{x}_0(\omega') \rangle + M_{12}(\omega') \langle \mathcal{F}\{y_0^n\}(\omega') \tilde{y}_0(\omega) \rangle] \}, \tag{A27}
\end{aligned}$$

grouping all terms proportional to $c_{A,n}$,

$$\begin{aligned}
& -k_I \int \frac{d\omega d\omega'}{2\pi^2} e^{it(\omega+\omega')}(i\omega') [M_{21}(\omega) \langle \mathcal{F}\{x_0^n\}(\omega) \tilde{x}_0(\omega') \rangle + M_{11}(\omega') \langle \mathcal{F}\{x_0^n\}(\omega') \tilde{y}_0(\omega) \rangle] \\
& = -k_I n!! (\sigma_{mA} T_m + \sigma_A T_A)^{\frac{n-1}{2}} \int \frac{d\omega d\omega' d\omega_n}{(2\pi)^2} e^{it(\omega+\omega')}(i\omega') \delta(\omega + \omega') [M_{21}(\omega) \langle \tilde{x}_0(\omega_n) \tilde{x}_0(\omega') \rangle + M_{11}(\omega') \langle \tilde{x}_0(\omega_n) \tilde{y}_0(\omega) \rangle] \\
& = -k_I n!! (\sigma_{mA} T_m + \sigma_A T_A)^{\frac{n-1}{2}} \int \frac{d\omega' d\omega_n}{(2\pi)^2} (i\omega') [M_{21}(-\omega') \langle \tilde{x}_0(\omega_n) \tilde{x}_0(\omega') \rangle + M_{11}(\omega') \langle \tilde{x}_0(\omega_n) \tilde{y}_0(-\omega') \rangle] \\
& = n!! \kappa_0 \beta_A (\sigma_{mA} T_m + \sigma_A T_A)^{\frac{n-1}{2}} (T_A - T_B), \tag{A28}
\end{aligned}$$

and to $c_{B,n}$,

$$\begin{aligned}
& -k_I \int \frac{d\omega d\omega'}{2\pi^2} e^{it(\omega+\omega')}(i\omega') [M_{22}(\omega) \langle \mathcal{F}\{y_0^n\}(\omega) \tilde{x}_0(\omega') \rangle + M_{12}(\omega') \langle \mathcal{F}\{y_0^n\}(\omega') \tilde{y}_0(\omega) \rangle] \\
& = -k_I n!! (\sigma_{mB} T_m + \sigma_B T_B)^{\frac{n-1}{2}} \int \frac{d\omega d\omega' d\omega_n}{(2\pi)^2} e^{it(\omega+\omega')}(i\omega') \delta(\omega + \omega') [M_{22}(\omega) \langle \tilde{y}_0(\omega_n) \tilde{x}_0(\omega') \rangle + M_{12}(\omega') \langle \tilde{y}_0(\omega_n) \tilde{y}_0(\omega) \rangle] \\
& = -k_I n!! (T_m \sigma_{mB} + \sigma_B T_B)^{\frac{n-1}{2}} \int \frac{d\omega' d\omega_n}{(2\pi)^2} (i\omega') [M_{22}(-\omega') \langle \tilde{y}_0(\omega_n) \tilde{x}_0(\omega') \rangle + M_{12}(\omega') \langle \tilde{y}_0(\omega_n) \tilde{y}_0(-\omega') \rangle] \\
& = n!! \kappa_0 \beta_B (\sigma_{mB} T_m + \sigma_B T_B)^{\frac{n-1}{2}} (T_A - T_B), \tag{A29}
\end{aligned}$$

finally yielding the first-order correction

$$\begin{aligned}
J_1 & = \kappa_0 \beta_A \sum_n [c_n^A n!! (\sigma_{mA} T_m + \sigma_A T_A)^{\frac{n-1}{2}}] (T_A - T_B) + \kappa_0 \beta_B \sum_n [c_n^B n!! (\sigma_{mB} T_m + \sigma_B T_B)^{\frac{n-1}{2}}] (T_A - T_B) \\
& \equiv \kappa_0 [\beta_A g_A (\sigma_{mA} T_m + \sigma_A T_A) + \beta_B g_B (\sigma_{mB} T_m + \sigma_B T_B)] (T_A - T_B), \tag{A30}
\end{aligned}$$

where we have defined

$$g_j(z) = \sum_n c_{j,n} n!! z^{\frac{n-1}{2}}, \tag{A31}$$

for $j = A, B$. Examples of the correspondence between g_j and the force f_j are given in Table I.

Moreover, recall that κ_0 was defined in Eq. (18), and the remaining coefficients in Eq. (A30) were defined in Eqs. (A21), (A22), (A28), and (A29). Their, explicit values for the particular case $m_A = m_B = m$, $\gamma_A = \gamma_B = \gamma$, additionally defining $\bar{m} = m/\gamma^2$, are given below:

$$\kappa_0 = \frac{2k_I^2/\gamma}{[4k_I^2 + (k_A - k_B)^2] \bar{m} + 2(k_A + k_B + 2k_I)}, \tag{A32}$$

$$\sigma_{mA} = \sigma_{mB} = \sigma_m = \frac{2k_I^2 [(2k_I + k_A + k_B) \bar{m} + 2]}{[k_A k_B + k_I (k_A + k_B)] \{ [4k_I^2 + (k_A - k_B)^2] \bar{m} + 2[2k_I + k_A + k_B] \}}, \tag{A33}$$

$$\sigma_A = \frac{(k_A - k_B) [(k_A - k_B)(k_B + k_I) - 2k_I^2] \bar{m} + 2[k_B(k_A + k_B) + k_I(k_A + 3k_B)]}{[k_A k_B + k_I(k_A + k_B)] \{ [4k_I^2 + (k_A - k_B)^2] \bar{m} + 2[2k_I + k_A + k_B] \}}, \tag{A34}$$

$$\sigma_B = \frac{(k_B - k_A) [(k_B - k_A)(k_A + k_I) - 2k_I^2] \bar{m} + 2[k_A(k_A + k_B) + k_I(k_B + 3k_A)]}{[k_A k_B + k_I(k_A + k_B)] \{ [4k_I^2 + (k_A - k_B)^2] \bar{m} + 2[2k_I + k_A + k_B] \}}, \tag{A35}$$

$$\beta_A = \frac{2[1 + \bar{m}(k_A - k_B)]}{[4k_I^2 + (k_A - k_B)^2] \bar{m} + 2(2k_I + k_A + k_B)}, \tag{A36}$$

$$\beta_B = \frac{2[1 - \bar{m}(k_B - k_A)]}{[4k_I^2 + (k_A - k_B)^2] \bar{m} + 2(2k_I + k_A + k_B)}. \tag{A37}$$

3. Heat flow in the small- k_I regime

Since we are interested in the regime of very small k_I , we can suppress the contributions of $\sigma_{mA} \sim O(k_I^2)$ and $\sigma_{mB} \sim O(k_I^2)$, since $\sigma_A \sim O(k_I^0)$ and $\sigma_B \sim O(k_I^0)$, leading to

$$J_1 \simeq \kappa_0 [\beta_A g_A (\sigma_A T_A) + \beta_B g_B (\sigma_B T_B)] (T_A - T_B). \tag{A38}$$

Below, we write the explicit expressions of all the coefficients for three especial cases, where the asymmetry relies either on the spring constant, the mass or damping parameter.

a. Different stiffness

Assuming $m_A = m_B = m$ and $\gamma_A = \gamma_B = \gamma$:

$$\kappa_0 = \frac{2\gamma k_I^2}{(k_A - k_B)^2 m + 2(k_A + k_B)\gamma^2}, \quad (\text{A39})$$

$$\sigma_A = \frac{1}{k_A}, \quad (\text{A40})$$

$$\sigma_B = \frac{1}{k_B}, \quad (\text{A41})$$

$$\beta_A = \frac{2[(k_A - k_B)m + \gamma^2]}{(k_A - k_B)^2 m + 2(k_A + k_B)\gamma^2}, \quad (\text{A42})$$

$$\beta_B = \frac{2[(k_B - k_A)m + \gamma^2]}{(k_A - k_B)^2 m + 2(k_A + k_B)\gamma^2}. \quad (\text{A43})$$

b. Different damping

Assuming $m_A = m_B = m$ and $k_A = k_B = k$:

$$\kappa_0 = \frac{k_I^2}{k(\gamma_A + \gamma_B)}, \quad (\text{A44})$$

$$\sigma_A = \sigma_B = \frac{1}{k}, \quad (\text{A45})$$

$$\beta_A = \frac{\gamma_B}{k(\gamma_A + \gamma_B)}, \quad (\text{A46})$$

$$\beta_B = \frac{\gamma_A}{k(\gamma_A + \gamma_B)}. \quad (\text{A47})$$

c. Different mass

Assuming $\gamma_A = \gamma_B = \gamma$ and $k_A = k_B = k$:

$$\kappa_0 = \frac{\gamma(m_A + m_B)k_I^2}{k[k(m_A - m_B)^2 + 2(m_A + m_B)\gamma^2]}, \quad (\text{A48})$$

$$\sigma_A = \sigma_B = \frac{1}{k}, \quad (\text{A49})$$

$$\beta_A = \frac{2k(m_B - m_A)m_B + (m_A + m_B)\gamma^2}{k[k(m_A - m_B)^2 + 2(m_A + m_B)\gamma^2]}, \quad (\text{A50})$$

$$\beta_B = \frac{2k(m_A - m_B)m_A + (m_A + m_B)\gamma^2}{k[k(m_A - m_B)^2 + 2(m_A + m_B)\gamma^2]}. \quad (\text{A51})$$

-
- [1] F. Bonetto, J. L. Lebowitz, and L. Rey-Bellet, Fourier's Law: A challenge for theorists, *Math. Phys.* **2000**, 128 (2000).
- [2] S. Lepri, R. Livi, and A. Politi, Thermal conduction in classical low-dimensional lattices, *Phys. Rep.* **377**, 1 (2003).
- [3] A. Dhar, Heat transport in low-dimensional systems, *Adv. Phys.* **57**, 457 (2008).
- [4] S. Lepri, R. Livi, and A. Politi in *Thermal Transport in Low Dimensions: From Statistical Physics to Nanoscale Heat Transfer*, edited by S. Lepri (Springer International Publishing, New York, 2016), pp. 1–38.
- [5] C. W. Chang, D. Okawa, H. Garcia, A. Majumdar, and A. Zettl, Breakdown of Fourier's Law in Nanotube Thermal Conductors, *Phys. Rev. Lett.* **101**, 075903 (2008).
- [6] N. Yang, G. Zhang, and B. Li, Violation of Fourier's law and anomalous heat diffusion in silicon nanowires, *Nano Today* **5**, 85 (2010).
- [7] Z. Wang, J. A. Carter, A. Lagutchev, Y. K. Koh, N.-H. Seong, D. G. Cahill, and D. D. Dlott, Ultrafast flash thermal conductance of molecular chains, *Science* **317**, 787 (2007).
- [8] T. Meier, F. Menges, P. Nirmalraj, H. Hölscher, H. Riel, and B. Gotsmann, Length-Dependent Thermal Transport Along Molecular Chains, *Phys. Rev. Lett.* **113**, 060801 (2014).
- [9] N. Li, J. Ren, L. Wang, G. Zhang, P. Hänggi, and B. Li, Colloquium: Phononics: Manipulating heat flow with electronic analogs and beyond, *Rev. Mod. Phys.* **84**, 1045 (2012).
- [10] B. Li, L. Wang, and G. Casati, Thermal Diode: Rectification of Heat Flux, *Phys. Rev. Lett.* **93**, 184301 (2004).
- [11] C. W. Chang, D. Okawa, A. Majumdar, and A. Zettl, Solid-state thermal rectifier, *Science* **314**, 1121 (2006).
- [12] E. Pereira and R. R. Ávila, Increasing thermal rectification: Effects of long-range interactions, *Phys. Rev. E* **88**, 032139 (2013).

- [13] S. Chen, E. Pereira, and G. Casati, Ingredients for an efficient thermal diode, *Europhys. Lett.* **111**, 30004 (2015).
- [14] J. Wang and Z. Zheng, Heat conduction and reversed thermal diode: The interface effect, *Phys. Rev. E* **81**, 011114 (2010).
- [15] M. Pons, Y. Y. Cui, A. Ruschhaupt, M. A. Simón, and J. G. Muga, Local rectification of heat flux, *Europhys. Lett.* **119**, 64001 (2017).
- [16] S. Chen, D. Donadio, G. Benenti, and G. Casati, Efficient thermal diode with ballistic spacer, *Phys. Rev. E* **97**, 030101(R) (2018).
- [17] B. Li, J. Lan, and L. Wang, Interface Thermal Resistance Between Dissimilar Anharmonic Lattices, *Phys. Rev. Lett.* **95**, 104302 (2005).
- [18] L. Zhang, P. Keblinski, J.-S. Wang, and B. Li, Interfacial thermal transport in atomic junctions, *Phys. Rev. B* **83**, 064303 (2011).
- [19] E. Pereira Requisite ingredients for thermal rectification, *Phys. Rev. E* **96**, 012114 (2017).
- [20] N. Kalantar, B. K. Agarwalla, and D. Segal, Harmonic chains and the thermal diode effect, *Phys. Rev. E* **103**, 052130 (2021).
- [21] M. A. Simón, A. Alaña, M. Pons, A. Ruiz-García, and J. G. Muga, Heat rectification with a minimal model of two harmonic oscillators, *Phys. Rev. E* **103**, 012134 (2021).
- [22] S. Kaushik, S. Kaushik, and R. Marathe, Simple analytical model of a thermal diode, *Eur. Phys. J. B* **91**, 87 (2018).
- [23] C. KargI, M. T. Naseem, T. Opatrný, O. E. Müstecaplıođlu, and G. Kurizki, Quantum optical two-atom thermal diode, *Phys. Rev. E* **99**, 042121 (2019).
- [24] V. Balachandran, G. Benenti, E. Pereira, G. Casati, and D. Poletti, Perfect Diode in Quantum Spin Chains, *Phys. Rev. Lett.* **120**, 200603 (2018).
- [25] J. Verner, Explicit Runge-Kutta methods with estimates of the local truncation error, *SIAM J. Numer. Anal.* **15**, 772 (1978).
- [26] T. J. Alexander, High-heat-flux rectification due to a localized thermal diode, *Phys. Rev. E* **101**, 062122 (2020).
- [27] M. Romero-Bastida, J. O. M. Peña, and J. M. López, Thermal rectification in mass-graded next-nearest-neighbor Fermi-Pasta-Ulam lattices, *Phys. Rev. E* **95**, 032146 (2017).
- [28] S. Liu, J. Liu, P. Hanggi, C. Wu, and B. Li, Triggering waves in nonlinear lattices: Quest for anharmonic phonons and corresponding mean-free paths, *Phys. Rev. B* **90**, 174304 (2014).